Decadal Changes in Soil and Atmosphere Temperature Differences Linked With Environment Shifts Over Northern Eurasia

Chen, Liangzhi

2021-03

Chen , L , Aalto , J & Luoto , M 2021 , ' Decadal Changes in Soil and Atmosphere Temperature Differences Linked With Environment Shifts Over Northern Eurasia ' , Journal of geophysical research. Earth surface , vol. 126 , no. 3 , ARTN e2020JF005865 . https://doi.org/10.1029/2020JF005

http://hdl.handle.net/10138/329028
https://doi.org/10.1029/2020JF005865

JGR Earth Surface

RESEARCH ARTICLE
10.1029/2020JF005865

Decadal Changes in Soil and Atmosphere Temperature Differences Linked With Environment Shifts Over Northern Eurasia

Liangzhi Chen[1], **Juha Aalto**[1,2], **and Miska Luoto**[1]

[1]Department of Geosciences and Geography, University of Helsinki, Helsinki, Finland, [2]Finnish Meteorological Institute, Helsinki, Finland

Key Points:

- The study is the first view of the trend in soil-air temperature difference and its links with changing environment over northern Eurasia
- Discordance between trends in mean annual air and soil temperatures causes the varying temperature difference during 1981–2015
- Trends in temperature difference significantly respond to the altered snow cover, solar radiation, and soil moisture during the period

Supporting Information:

- Supporting Information S1

Correspondence to:
L. Chen,
liangzhi.chen@helsinki.fi

Citation:
Chen, L., Aalto, J., & Luoto, M. (2021). Decadal changes in soil and atmosphere temperature differences linked with environment shifts over northern Eurasia. *Journal of Geophysical Research: Earth Surface*, *126*, e2020JF005865. https://doi.org/10.1029/2020JF005865

Received 2 SEP 2020
Accepted 8 FEB 2021

Abstract The difference between soil and air temperatures (ΔT) in a specified time is dependent on meteorological conditions, properties of soil and land covers. Understanding ΔT is critical in assessing land–atmosphere thermal interactions in changing environment. However, systematic knowledge of interannual variations and responses of ΔT to the environmental changes (e.g., snow cover and soil moisture) at decadal scales remain limited. Here, variations of the mean annual air and soil temperatures, and ΔT were investigated at 217 sites in northern Eurasia during 1981–2015. It is found that changes in the mean annual air and soil temperatures were inconsistent as the average increase in soil temperature was generally less than that of air. The relationships between trends in soil and air temperatures were significant in the upper ground (0.2 and 0.8 m) over the seasonal frost region but insignificant in the permafrost regions and deeper ground. During the period, widespread changes in ΔT occurred and closely responded to the environmental changes, but the relationships varied with soil depth. Among the tested factors, trends in snow cover thickness dominantly control trends in ΔT, followed by trends in snow cover duration and solar radiation. Both linear and nonlinear analyses indicate enhanced relationships between trends in snow depth and ΔT as depth increases. This study provides the first view of decadal trends in ΔT and conjunctions with the environmental changes during 1981–2015 over northern Eurasia. The findings are relevant to quantify land–atmosphere thermal interactions given impacts of future environmental changes.

Plain Language Summary Environmental conditions affect the difference between soil–atmosphere temperatures in a specified period, for example the annual soil–atmosphere temperature difference (ΔT). However, knowledge of how ΔT has changed during the past few decades and its relations with changing snow cover, solar radiation, rainfall, soil moisture, and vegetation is insufficient. Here, we examined the trends in ΔT and linked them with the environmental changes during 1981–2015 over northern Eurasia. We found discordant warming rates in air and soil temperatures during the period, leading to extensive variations in ΔT, which significantly respond to multiple environmental changes. The changes in snow cover, solar radiation, and soil moisture significantly correlate with trends in ΔT, while vegetation and rainfall changes have less clear relations. The changes in snow cover thickness are more influential on trends in ΔT than that of snow cover duration. As the first one, this study provides a holistic view of long-term trends in ΔT and quantifies the role of changing environment at large space and time scales. The findings can enhance our understanding of the variability of land-atmosphere temperature difference in a changing environment. The work is also relevant for the research in ecosystem functions, roots development, and infrastructure stability under future climate.

1. Introduction

The soil temperature is an integrator of hydrothermal processes and their interactions near ground surface and within soil. Subsurface soil temperature differs from ambient air temperature by the presence of environmental elements, such as snow cover, vegetation, soil organic materials and moisture, and solar radiation (Aalto et al., 2018; Frenne et al., 2019; Grundstein et al., 2005; Lenoir et al., 2017; Zhang, 2005). The difference between soil and air temperatures (ΔT) substantially affects not only freeze–thaw depth of frost-related ground but also temperature-sensitive processes in biogeochemical and biogeophysical functions, such as soil carbon decomposition, vegetation growth, and snow cover retreat (Blunden & Arndt, 2019; Bokhorst

et al., 2016; Davidson & Janssens, 2006; Walther et al., 2002; Wang et al., 2011). Systematic interannual changes in environmental variables discord trends in the mean annual air and soil temperatures by introducing nonatmospheric trends to soil temperature records, and hence causes temporal variations of ΔT (Bulygina et al., 2011; García-García et al., 2016; González-Rouco et al., 2003; Grundstein et al., 2005; Peng et al., 2016; Romanovsky et al., 2007). However, long-term interannual variations of ΔT and its response to the changing environmental conditions are little known yet as most previous efforts have been devoted to ΔT and its controls at seasonal (or diurnal) scale (Aalto et al., 2018; Bartlett et al., 2004; Wang et al., 2017).

Examining trends in ΔT and the role of environmental changes at large spatiotemporal scales are challenging due to data limitation in terms of the consistency and spatiotemporal coverage of observations. Thus, it has constrained only partial characterizations from case studies in short periods or by excluding key elements as snow cover has received more attention while, e.g., vegetation and soil moisture are rarely addressed simultaneously (Bartlett et al., 2004; Hrbáček et al., 2016; Jungqvist et al., 2014; Yazaki et al., 2013; Zhang, 2005). In northern Eurasia, multidepth soil temperatures and snow cover depth have been documented for decades, enabling us to investigate the interannual variability of ΔT at a large spatiotemporal scale.

Northern Eurasia is a key part of the global earth system, and regional climate warming is greater than the global average accompanied by increased frequency and intensity of extreme weather events (Blunden & Arndt, 2019; Groisman et al., 2016; Papalexiou & Montanari, 2019). The weather extremes even have prolonged impacts and feedback to land–atmosphere thermal interactions after taking place (Knapp et al., 2008). Previous attention has been mostly paid to ΔT between air and topsoil temperatures (<0.2 m) (Aalto et al., 2018; Bartlett et al., 2004; Luo et al., 2018; Zhang et al., 2018). In contrast, the knowledge of ΔT between air and deeper ground (>0.2 m) remains limited and is also of great importance as over half of soil carbon out of 2,344 Gt C at depths of up to 3 m is stocked in 0.2–2.0 m layer (Jobbágy & Jackson, 2000). Moreover, in frost-related regions, soil carbon decomposition in the deeper ground may proceed more rapidly than the upper under a warming climate (Bernal et al., 2016; Koven et al., 2015). Thus, examining long-term trends in ΔT and, in conjunction with the environmental changes, are essential in assessing land-climate thermal interactions under a changing climate.

Here, we provide the first holistic view of observed trends in ΔT at multiple soil depths and environmental variables at 217 sites in northern Eurasia during 1981–2015. Further, we use statistical methods to investigate links between trends in ΔT and environmental variables, including snow cover, rainfall, solar radiation, vegetation, and soil moisture during the period.

2. Materials and Methods

2.1. Data Compilation

We extracted daily air and soil temperatures, snow depth, and rainfall observations collected during 1981–2015 at weather stations operated by the All-Russia Research Institute of Hydrometeorological Information – World Data Center (RIHMI-WDC). The observation network covers the majority of land in northern Eurasia at latitudes from 42 to 70°N and longitudes from 28 to 170°E (Figure 1). The air temperature was measured 2 meters above ground, and soil temperatures were measured under natural cover of grasses and snow at depths of 0.2, 0.8, and 1.6 m (Gilichinsky et al., 1998). The measurement accuracies of temperatures and snow depth are within 0.1°C and 0.1 cm, respectively. Both datasets were released to the public after extensive quality control checks, and only qualified data were used in the study (Text S1 and Table S1) (Bulygina & Razuvaev, 2012; Sherstiukov, 2012).

The daily measurements were then computed into annual values: mean annual soil temperature (MAST), mean annual air temperature (MAAT), the annual rainfall (Rainfall, liquid precipitation), the annual mean of daily snow depth (AMSD, an average of daily snow depth during a year), snow cover duration (SCD, a sum of the days that snow exists during a year). In computing annual values, we defined a qualified year as a calendar year, during which at least 300-day data are available. On average, there are over 360-day measurements available for computing annual values in the datasets (full summary in Table S2). Apart from in situ observations, we extracted monthly gridded (9 km spatial resolution) attributes from ERA5–Land products, which were then computed to annual values: surface net solar radiation (SolarRad, absorbed solar

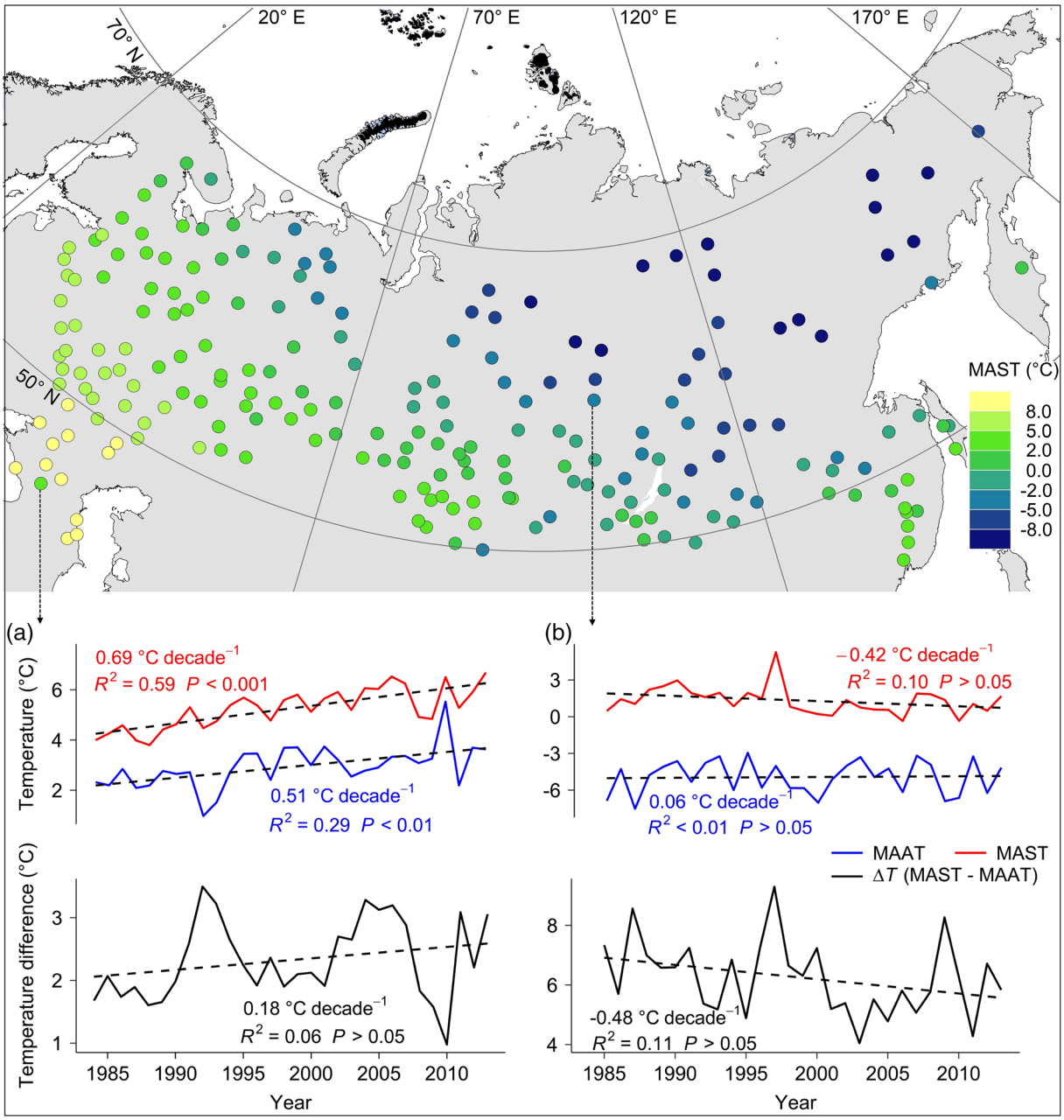

Figure 1. Map of 217 sites and corresponding mean annual soil temperature (MAST, 0.2 m) during 1981–2015. (a)–(b) show that distinct trends in MAST and mean annual air temperature (MAAT) lead to reversed trends in the annual soil-atmosphere temperature difference (ΔT) at two locations (a. Shadzhatmaz, (b) Vanavara). ΔT is defined as the arithmetic difference between MAST and MAAT (ΔT = MAST – MAAT). Trends (dashed lines) are based on linear least squares regressions, and corresponding statistics are presented.

radiation), leaf area index (LAI), volumetric water content (VWC, including the ice content) (Hersbach et al., 2020). The VWC is available at three layers (VWC $_{0.2}$, VWC$_{0.8}$, and VWC$_{1.6}$, corresponding to soil depth intervals of 0–0.2 m, 0–0.8 m, and 0–1.6 m, respectively).

2.2. Data Processing and Analyses

We investigated trends in air, soil temperatures, and other environmental variables during 1981–2015. Trends in individual variables were calculated as the slopes of linear least squares regressions at each location. The criteria in computing trends are the following; 1). A station has to have a minimum of 10-year

qualified data. 2). At least 90% of the years are needed during computing period (for example, if observations at a station spanned across 10 years during 1981–1990, at least 9-year data are needed for computing trends). 3). Trends of all variables were calculated in a common set of years for consistency in analyses. We then defined the annual difference (ΔT, °C) between MAST and MAAT as (Figure 1):

$$\Delta T = \text{MAST} - \text{MAAT}$$

We examined trends in ΔT ($\Delta T_{0.2}$, $\Delta T_{0.8}$, and $\Delta T_{1.6}$), which is derived from MAAT and MASTs at multiple soil depths (0.2, 0.8, and 1.6 m). In total, we assembled 184, 194, and 196 sites in calculating trends of $\Delta T_{0.2}$, $\Delta T_{0.8}$, and $\Delta T_{1.6}$, respectively, due to the different availabilities of soil temperature data with depth. The average numbers of years used for calculating trends range from 27.4 to 30.2 years at depths during 1981–2015 (details in Figure S1).

Then, trends in ΔT were linked to the environmental changes by generalized additive mixed model (GAMM). Unlike linear regression, GAMM captures the impact of changing environment on ΔT trends by smooth functions, which can be linear or nonlinear depending on the underlying patterns in the data (Text S2) (Hastie & Tibshirani, 1990; Wood, 2017). The number of years was included as a random term because of the different years used for computing trends at the sites (Figure S1). The collinearity diagnostics by multiple indices including pairwise correlations, condition index (CI) (Belsley et al., 2005; Douglass et al., 2003), variance inflation factor (VIF) (Hair et al., 1995), and tolerance suggest that no highly correlated variables were included in the models (Table S3, Figure S2) (Dormann et al., 2013). The response curves of trends in ΔT and other variables were fitted and optimized by the restricted maximum likelihood method (REML) (Patterson & Thompson, 1971; Wood, 2017) and visualized with 95% confidence intervals. The statistical significance of each variable across models is reported by three levels: very significant: $p \leq 0.001$; significant $0.001 < p \leq 0.05$; insignificant; $p > 0.05$. The detailed summary statistics of models are available in Table S4. To characterize the contribution of each variable in the models, we use Pearson correlation coefficient between fitted values of the models and predictions where the variable under investigation has been randomly permutated (Breiman, 2001; Thuiller et al., 2009). Then, the importance of the variable is simply calculated by the following equation:

$$\text{Variable importance} = 1 - |\text{Pearson correlation}(\text{prediction}_{\text{original varaible}}, \text{prediction}_{\text{one variable permutated}})|$$

Consequently, the magnitude of variable importance is constrained from 0 to 1, in which the higher, the more influential the variable is. Finally, the variable importance was averaged over 100 permutations with an error bar representing a 95% confidence interval over the permutations. All analyses were undertaken on R platform (v.3.6.3) (R core team, 2017) with packages of ggplot2 (Wickham, Chang, et al., 2020), ggpubr (Kassambara, 2020), dplyr (Wickham, François, et al., 2020), cowplot (Wilke, 2019), mgcv (Wood, 2019), mgcViz (Fasiolo et al., 2020), biomod2 (Thuiller et al., 2020).

3. Results

3.1. Trends in Air and Soil Temperatures From 1981 to 2015

The increases in soil and air temperatures during 1981–2015 were significant and varied spatially (Figures 2a–2d). For the region as a whole, warming rate of soil temperature at 0.2 m by 0.36 ± 0.03°C decade^{-1} (Mean ± standard error of the mean) was greater than the deeper ground (1.6 m, 0.27 ± 0.02°C decade^{-1}). The increase in air temperature at 0.34 ± 0.01°C decade^{-1} was slightly less than soil warming at 0.2 m but greater than the warming in the deeper ground. Regionally, increases in soil temperatures at multiple depths were generally less than that of air temperature except at a depth of 0.2 m in the seasonal frost region. Of note, in the discontinuous permafrost region, the warming rate of soil temperature at 0.2 m was only about half of that of air; however, soil temperatures warmed at a similar rate to air temperature at greater depth. This difference can be attributed to the latent heat effects due to freeze–thaw cycles of water, which is more significant close to the surface than at greater depth. Therefore, change in MAAT cannot account for the warming of MASTs with depth and such inconsistency consequently caused interannual variations in ΔT during the period.

The linear relationships indicate that trends in air and soil temperatures at 0.2 and 0.8 m were significantly related over the seasonal frost region (Figure 3 and Table 1). However, in the permafrost regions and a

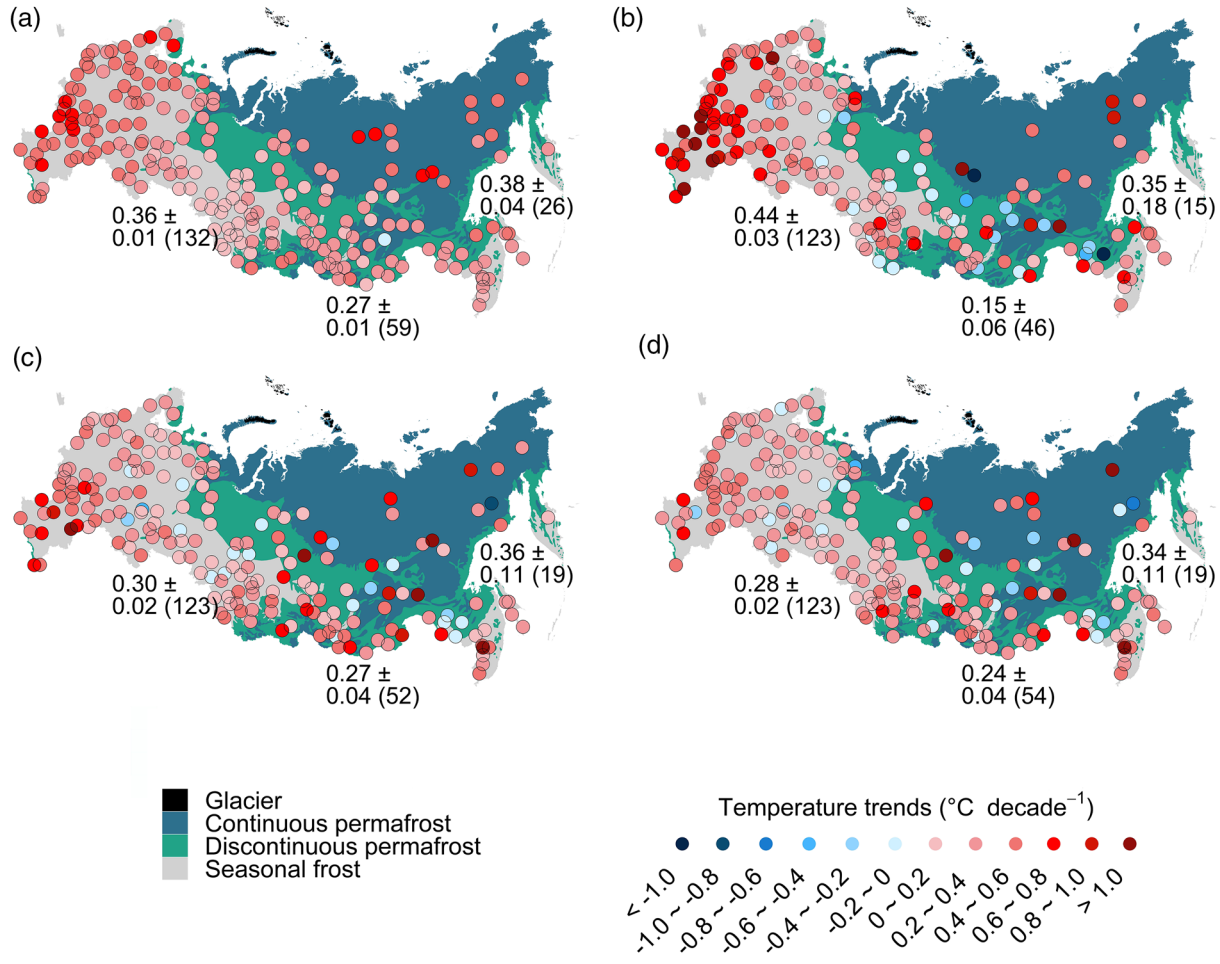

Figure 2. Distribution of trends in MAAT (a) and MASTs at depths of 0.2 (b), 0.8 (c), and 1.6 m (d) during 1981–2015. The numbers represent the mean trends and standard error of the mean (SEM) in the regions of continuous permafrost (right), discontinuous permafrost (bottom), and seasonal frost (left), respectively. The total numbers of sites are reported in brackets. The extent of frozen ground (Continuous permafrost region (extent of permafrost ≥ 90%), Discontinuous permafrost region (0% < extent of permafrost < 90%)) is derived from permafrost map of the International Permafrost Association (Brown et al., 1997).

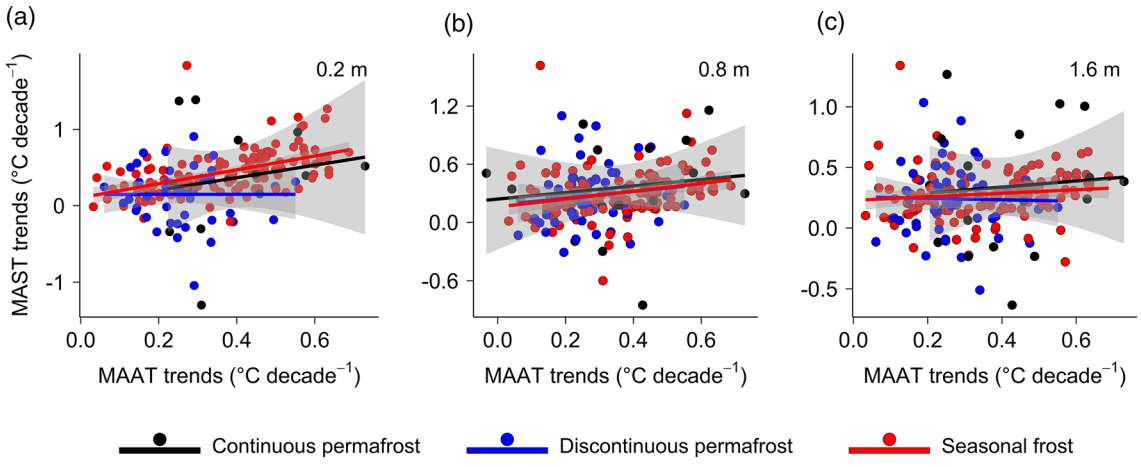

Figure 3. Linear relationships between the trends in MAAT and MASTs at depths of 0.2 (a), 0.8 (b), and 1.6 m (c). Points are shaded according to the extent of frozen ground. Fitted lines with 95% confidence bands are based on linear least squares regressions. Detailed statistics of regressions are shown in Table 1.

deeper depth (1.6 m), there were no clear relationships between trends in air and soil temperatures. In the region as a whole, the relationships between trends in soil and air temperature were significant at depths of 0.2 and 0.8 m, and insignificant at 1.6 m.

3.2. Decadal Trends in ΔT during 1981–2015

Although the average trends in ΔT are slightly below the null (0°C decade^{-1}) at multiple depths, they are spatially heterogeneous across 217 sites (Figure 4). For example, trends in $\Delta T_{0.2}$ show the greatest ranging from −2.3 to over 1.0°C decade^{-1} while similar variability can be found in trends of $\Delta T_{0.8}$ and $\Delta T_{1.6.}$ Across the entire region, trends in ΔT in the upper ground decrease from south to north as they significantly relate to the latitudes of locations (Figures 5c and 5d). As depth increases, the relationship between trends in ΔT and latitude diminishes and becomes less significant. There are no clear relationships between trends in ΔT and MASTs ($p > 0.1$), whereas trends in ΔT account for 0.7 of the trends in MAST at 0.2 m and account less in the deeper ground (0.8 and 1.6 m) (Figures 5a–5d).

3.3. Linear Relationships Between Trends in ΔT and Environmental Variables

The environmental conditions in the area have changed over the past few decades. Snow characteristics have changed, including a minor increase in AMSD (0.06 ± 0.08 cm decade^{-1}, Mean ± SEM) but decrease in SCD (−2.39 ± 0.23 days decade^{-1}) (Figures 6a, S3a and S3b). The reversed changes between the two snow parameters demonstrate previous studies on increased snowfall extremes and maximum snow depth in the area (Bulygina et al., 2011; Donat et al., 2016). SolarRad has widely increased at over 95% sites with an average of 0.06 w m^{-2} decade^{-1} (Figures 6a and Figure S3c). Annual rainfall also significantly increased on an average of 5.20 ± 1.20 mm decade^{-1} (Figures 6a and S3d). Nevertheless, soil moisture loss is significant at multiple depths over the region, which is likely attributable to the alterations in the evaporation rate and infiltration of soil moisture to the deeper ground (Figures 6a, S3e–S3g, and S4) (Andresen et al., 2020).

Linear regressions demonstrate that trends in AMSD and SCD have significant relationships with trends in ΔT (Table 2). At a depth of 0.2 m, trends in SCD and AMSD explain the variance of ΔT trends at a similar level, while trends in SCD has a greater agreement with ΔT trends at 0.8 m than AMSD. The opposite can be found at 1.6 m, where trends in AMSD explain 30.4 % variance of ΔT trends, which is more than three times the variance attributed to SCD trends (10.0%). Trends in ΔT at 0.2 m significantly relate to trends in SolarRad, but the relationships are not significant at the deeper ground. There are no clear relationships between trends in LAI or Rainfall and ΔT. However, responses of ΔT to the changes in VWC are significant at depths of 0.2 and 0.8, but not at 1.6 m.

3.4. Trends in ΔT Linked With the Environmental Changes

To link decadal trends in ΔT and the changing environmental variables, we ran general additive mixed regression models with trends in environmental variables (AMSD, SCD, SolarRad, Rainfall, VWC, and LAI) as fixed smooth terms and the number of years used for computing trends as a random-effect term. It is noted that relationships between observed trends in variables and ΔT are nonlinear, suggesting that results from GAMMs are potentially more robust than the results from linear regressions that cannot capture nonlinear relationships due to the nature of the method (Figures 6b–6d). For example, GAMMs indicate significant relationships between trends in SolarRad and $\Delta T_{0.8}/\Delta T_{1.6}$, which, however, are not reflected by linear regressions (Figures 6b–6d and Table 2). Similarly, trend in $\Delta T_{1.6}$ significantly responds to VWC trend from GAMM but not as significant in linear regressions.

Trends in ΔT at multiple depths significantly relate to trends in environmental variables by explained variances ranging from 0.38 to 0.56 (Figure 6 and Table S4). Trends in ΔT are primarily attributed to the snow cover changes. Trends in AMSD are more influential at the deeper ground with over twofold variable importance of $\Delta T_{1.6}$ trends (0.79 ± 0.006, Mean ± 0.95 CI) than that in $\Delta T_{0.2}$ (0.31 ± 0.003), which agrees with linear analyses (Table 2 and Figure 6e). Of note, the negative trends in ΔT (meaning soil–atmosphere temperature difference became smaller) associate with the decrease in AMSD consistently and a turnover (negative to positive) of trends in ΔT occurs along with a shift of trend from decreasing to increasing

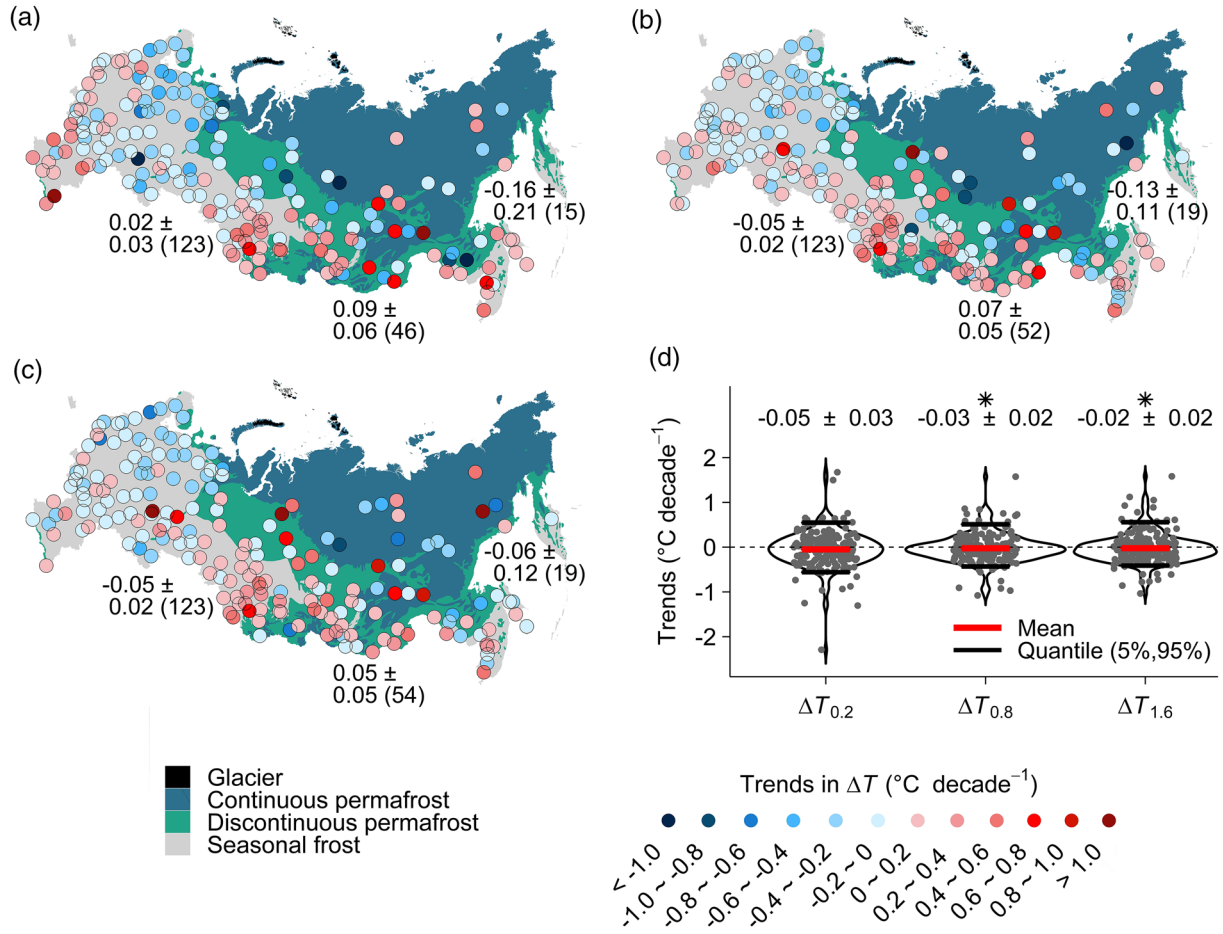

Figure 4. Distribution of trends in ΔT at 0.2 (a), 0.8 (b), and 1.6 m (c) during 1981–2015. The numbers represent mean trends and standard error of the mean (SEM) in regions of continuous permafrost (right), discontinuous permafrost (bottom), and seasonal frost (left), respectively. The numbers of sites are reported in brackets. (d). Violin plots display the densities of trends over the sites. Solid red and black lines depict trends on average and percentiles (5th and 95th), respectively. Averaged trends (Mean ± SEM) are reported at the top. The significance of averaged trends against null (representing no change: 0°C decade^{-1}) was tested by the Wilcoxon method and marked with Asterisks ($p < 0.05$) at the top.

AMSD. Compared with trends in AMSD, the relationships between trends in ΔT and SCD are flatter but still significant.

Trends in SolarRad significantly relate to trends in ΔT at multiple depths, and the influences decrease with depth (Figures 6b–6d). Trend in rainfall is the second influential factor for $\Delta T_{0.2}$ trend, while the relationships at other soil depths are not as clear. Notably, trends in SolarRad and rainfall poorly explain positive ΔT trends as curves are mostly below the null (Figures 6b–6d). In contrast, trends in soil VWC have significant nonlinear relationships with ΔT trends at all depths, but the response curves are mainly above the null. Moreover, trends in ΔT and LAI are less related with large uncertainties, but the relationship at a depth of 1.6 m is significant and negative, suggesting greening of vegetation may be a contributor to the decrease in $\Delta T_{1.6}$ by cooling ground even under a warming climate. In contrast, such relationships are less significant in the upper ground at decadal scales.

4. Discussion

The increase in the mean annual air and soil temperatures occurred at 217 sites in northern Eurasia during 1981–2015. The average increase in mean annual soil temperature is slightly lower than the increase in mean annual air temperature except at a depth of 0.2 m (0.44°C decade^{-1}), which is greater than the mean annual air temperature increase (0.36°C decade^{-1}) in the seasonal frost region (Figure 2). Such discordance

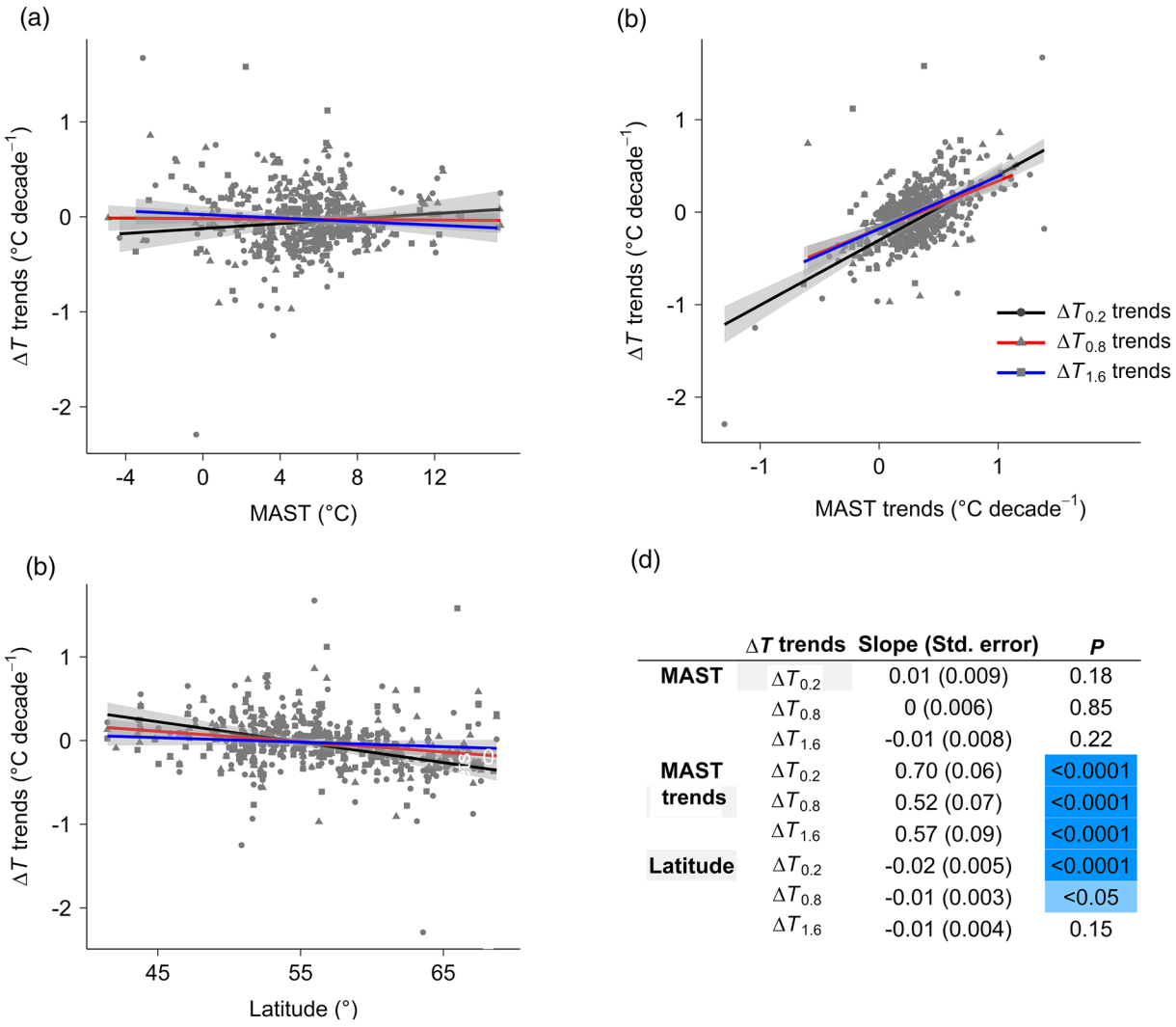

(d)

	ΔT trends	Slope (Std. error)	P
MAST	$\Delta T_{0.2}$	0.01 (0.009)	0.18
	$\Delta T_{0.8}$	0 (0.006)	0.85
	$\Delta T_{1.6}$	-0.01 (0.008)	0.22
MAST trends	$\Delta T_{0.2}$	0.70 (0.06)	<0.0001
	$\Delta T_{0.8}$	0.52 (0.07)	<0.0001
	$\Delta T_{1.6}$	0.57 (0.09)	<0.0001
Latitude	$\Delta T_{0.2}$	-0.02 (0.005)	<0.0001
	$\Delta T_{0.8}$	-0.01 (0.003)	<0.05
	$\Delta T_{1.6}$	-0.01 (0.004)	0.15

Figure 5. (a)–(c). Relationships between trends in ΔT and MAST (a), MAST trends (b), latitude (c) over the sites. Fitted lines with 95% confidence bands are based on linear regressions. (d). The table shows regression slopes (with standard error) and *p*-values (t-test) derived from figures (a)–(c).

between trends in air and soil temperatures demonstrates that air temperature change alone cannot explain soil warming over the region, consequently causing interannual variations of ΔT (Figure 2). It is found that trends in ΔT are spatially heterogeneous and significantly respond to trends in environmental variables, especially snow cover, solar radiation, and soil moisture.

The role of snow cover in decoupling soil and air temperatures has been widely examined (Chen et al., 2021; Romanovsky et al., 2007; Wang et al., 2017). Snow cover generally insulates the ground from coldness due to low thermal conductivity, whereas it does not always warm ground since long-lasting snow cover till next spring (or even summer) could have an overall cooling effect because of the albedo and energy required to melt its pack (Zhang, 2005). Nevertheless, the impacts of the different snow cover parameters (snow cover thickness and duration) on ground temperature are relatively poorly quantified yet (Isaksen et al., 2011). A modeling study by Bartlett et al. (2004) suggests that snow layer thickness is less critical than snow cover duration in modulating the mean annual surface ground temperature, while Romanovsky et al. (2007) highlights the influence of snow cover thickness on the mean annual soil temperature (at a depth of 1.6 m). We highlight that trends in ΔT have closer linear relationships with trends in AMSD than SCD except at depths of 0.2 and 0.8 m in the discontinuous and continuous permafrost regions, respectively (Table 2). In the whole area, trends in AMSD ($R^2 = 0.304$) account for three times

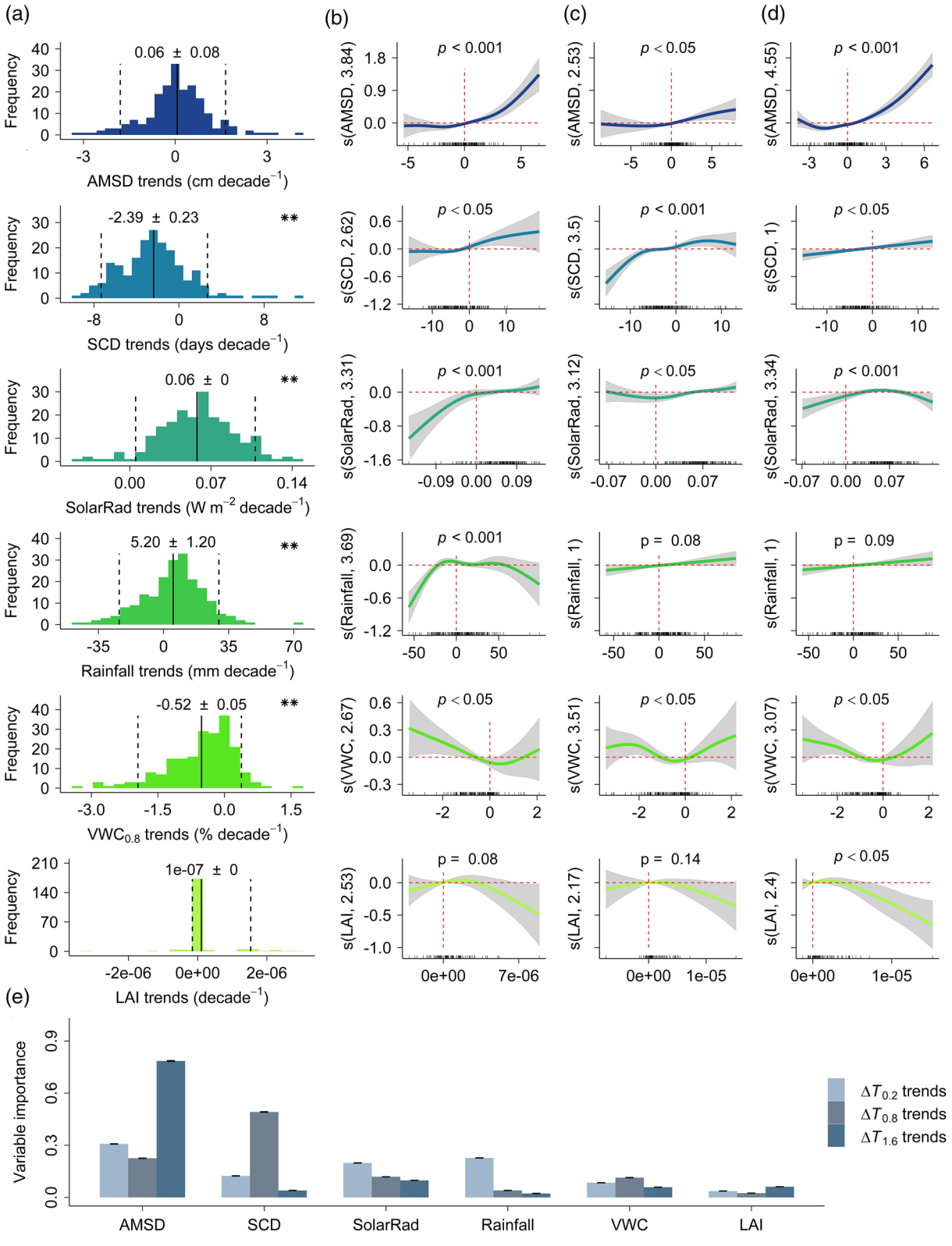
(a)
(b)
(c)
(d)
Frequency
0.06 ± 0.08
AMSD trends (cm decade^{-1})
-2.39 ± 0.23
**
SCD trends (days decade^{-1})
0.06 ± 0
SolarRad trends (W m^{-2} decade^{-1})
5.20 ± 1.20
Rainfall trends (mm decade^{-1})
-0.52 ± 0.05
VWC$_{0.8}$ trends (% decade^{-1})
1e-07 ± 0
LAI trends (decade^{-1})
s(AMSD, 3.84)
p < 0.001
s(AMSD, 2.53)
p < 0.05
s(AMSD, 4.55)
p < 0.001
s(SCD, 2.62)
p < 0.05
s(SCD, 3.5)
p < 0.001
s(SCD, 1)
p < 0.05
s(SolarRad, 3.31)
p < 0.001
s(SolarRad, 3.12)
p < 0.05
s(SolarRad, 3.34)
p < 0.001
s(Rainfall, 3.69)
p < 0.001
s(Rainfall, 1)
p = 0.08
s(Rainfall, 1)
p = 0.09
s(VWC, 2.67)
p < 0.05
s(VWC, 3.51)
p < 0.05
s(VWC, 3.07)
p < 0.05
s(LAI, 2.53)
p = 0.08
s(LAI, 2.17)
p = 0.14
s(LAI, 2.4)
p < 0.05
(e)
Variable importance
AMSD
SCD
SolarRad
Rainfall
VWC
LAI
$\Delta T_{0.2}$ trends
$\Delta T_{0.8}$ trends
$\Delta T_{1.6}$ trends

Table 1
Statistics of Linear Least Squares Regressions Between Trends in MAAT and MASTs and Permafrost extent.

Soil depth (m)	Extent of frozen ground	Slope (standard error)	*p*_value	*F*_statistics	R^2	N_{sites}
0.2	Seasonal frost	0.911 (0.16)	**< 0.0001**	**39.17**	0.245	123
	Discontinuous permafrost	0.002 (0.531)	0.997	< 0.01	< 0.001	46
	Continuous permafrost	0.821 (1.236)	0.518	0.441	0.033	15
	All frozen ground	0.953 (0.168)	**< 0.0001**	**32.19**	0.15	184
0.8	Seasonal frost	0.406 (0.134)	**0.003**	**9.107**	0.07	123
	Discontinuous permafrost	0.356 (0.428)	0.410	0.6897	0.014	52
	Continuous permafrost	0.335 (0.602)	0.585	0.3103	0.018	19
	All frozen ground	0.394 (0.133)	**0.003**	**8.797**	0.044	194
1.6	Seasonal frost	0.146 (0.113)	0.201	**1.653**	0.013	123
	Discontinuous permafrost	−0.062 (0.361)	0.864	0.030	0.001	54
	Continuous permafrost	0.249 (0.721)	0.735	0.119	0.007	19
	All frozen ground	0.163 (0.123)	0.184	**1.774**	0.009	196

Numbers in bold indicate significant relationships ($p < 0.05$).

greater variance of $\Delta T_{1.6}$ trends than trends in SCD ($R^2 = 0.100$), while a similar difference in variance of ΔT trends is observed at shallower depths. Meanwhile, nonlinear analyses by GAMM also suggest that ΔT trends more closely respond to trends in AMSD than SCD at three depths in the area. Moreover, both linear and nonlinear analyses indicate that changes in AMSD tend to be more influential on trends of ΔT in the deeper ground than the upper over northern Eurasia during 1981–2015 (Table 2 and Figure 6e).

Essentially, all variables affecting hydrothermal fluxes near the land–atmosphere interface and within the ground influence soil temperature. At middle and high latitudes, ΔT during the snow-free season is mainly governed by the amount of absorbed solar radiation, usually leading to warmer air temperature than soil temperature (Aalto et al., 2018; Bartlett et al., 2006; Putnam & Chapman, 1996). At an interannual time scale, our correlative analyses show that trends in ΔT are significantly related to the increase in SolarRad over the period in northern Eurasia (Figures 6a–6d). At a depth of 0.2 m, trend in SolarRad is the third important variable for explaining $\Delta T_{0.2}$ trend, which is at a similar level of trends in AMSD and rainfall, but not as important in the deeper ground (Figure 6e). The response curves for $\Delta T_{0.8}$ and $\Delta T_{1.6}$ are relatively flatter, whereas the decrease in SolarRad can explain the decrease in $\Delta T_{0.2}$ (Figures 6b–6d), suggesting that a decrease in SolarRad contributes to less warming of topsoil (0.2 m) temperature than air, but such influence dwindles at the deeper ground.

Annual rainfall has generally increased except at a small group of sites in the southern and southwestern parts of the area, which is in line with the previous studies (Bintanja & Andry, 2017; Groisman et al., 2016). Trends in rainfall have significant and nonlinear relationships with $\Delta T_{0.2}$ trends but not in the deeper ground (Figures 6b–6d). It is also noticeable that the response curve for trends of $\Delta T_{0.2}$ is largely below the null (trends in $\Delta T = 0$°C decade^{-1}), indicating that changes in rainfall barely explain the increase in ΔT (Figure 6b). The impacts of altered rainfall on soil temperature are complicated in terms of timing, frequency, and intensity. Peng et al. (2016) concluded that changes in rainfall might both negatively or positively affect trends in soil temperature across multiple models. Although annual rainfall has a slight effect on

Figure 6. (a). Histograms display trends in environmental variables at 217 sites during 1981–2015 ($VWC_{0.2}$ and $VWC_{1.6}$. In Figure S4). Trends in (a) are derived during the years without the constraint of data availability of ΔT, and the spatial variations of trends are shown in Figure S3. Average trends are reported with standard error of the mean (SEM) (Mean ± SEM) in subplots. Dashed lines indicate the 5th and 95th percentiles. The significance of averaged trend against null was tested by Wilcoxon method and marked with Asterisks that none (or two) indicate $p > 0.05$ (or $p < 0.0001$). Figures (b)–(d) show response curves between trends in ΔT (b. $\Delta T_{0.2}$; (c) $\Delta T_{0.8}$; (d) $\Delta T_{1.6}$) and environmental variables based on generalized additive mixed model (GAMM). The numbers in titles of *x*-axes represent the degree of freedom for model terms and are optimized and diagnosed to minimize overfitting or underfitting of the models (Text S2). Shades represent 95% confidence intervals and red dashed lines ($y = 0$ and $x = 0$) indicate nulls. Figure (e) shows relative importance for each variable with a 95% confidence bar over 100 permutations (full methodology in the methods).

Table 2
Summary Statistics of Relationships Between Trends in ΔT and Six Environmental Variables Estimated Using Linear Regression.

	Extent of frozen ground	AMSD	SCD	SolarRad	Rainfall	LAI	VWC
$\Delta T_{0.2}$	Seasonal frost	**0.154 (< 0.001)**	**0.087 (< 0.001)**	< 0.001 (0.860)	0.010 (0.283)	0.029 (0.065)	0.025 (0.088)
	Discontinuous permafrost	0.024 (0.307)	**0.208 (< 0.05)**	0.062 (0.099)	0.032 (0.238)	0.035 (0.217)	0.071 (0.076)
	Continuous permafrost	0.001 (0.918)	0.016 (0.672)	0.121 (0.223)	0.088 (0.304)	0.026 (0.584)	0.014 (0.683)
	All frozen ground	**0.034 (< 0.05)**	**0.046 (< 0.05)**	**0.030 (< 0.05)**	0.001 (0.650)	< 0.001 (0.986)	**0.031 (< 0.05)**
$\Delta T_{0.8}$	Seasonal frost	**0.206 (< 0.001)**	**0.135 (< 0.001)**	0.006 (0.393)	0.002 (0.657)	0.005 (0.457)	0.023 (0.097)
	Discontinuous permafrost	**0.189 (< 0.05)**	**0.155 (0.005)**	0.016 (0.388)	< 0.001 (0.946)	< 0.001 (0.997)	**0.096 (< 0.05)**
	Continuous permafrost	0.017 (0.640)	**0.509 (0.003)**	0.026 (0.563)	0.003 (0.836)	0.015 (0.665)	0.066 (0.354)
	All frozen ground	**0.148 (< 0.001)**	**0.191 (< 0.001)**	< 0.001 (0.900)	< 0.001 (0.910)	0.001 (0.690)	**0.022 (< 0.05)**
$\Delta T_{1.6}$	Seasonal frost	**0.337 (< 0.001)**	**0.186 (< 0.001)**	**0.044 (< 0.05)**	< 0.001 (0.971)	0.007 (0.375)	0.015 (0.185)
	Discontinuous permafrost	**0.277 (< 0.001)**	0.011 (0.466)	0.049 (0.122)	0.061 (0.084)	0.058 (0.091)	0.001 (0.841)
	Continuous permafrost	0.247 (0.101)	0.142 (0.227)	0.227 (0.118)	0.036 (0.558)	0.018 (0.678)	0.035 (0.559)
	All frozen ground	**0.304 (< 0.001)**	**0.100 (< 0.001)**	0.016 (0.090)	0.008 (0.227)	0.005 (0.340)	0.003 (0.477)

The coefficient of determination (R2) is reported with a statistical significance level (p) in the bracket. The significant relationships ($p < 0.05$) are in bold.

annual soil temperature (Karjalainen et al., 2019; Knight et al., 2018), Zhang et al. (2001) suggested that the changes in rainfall during summer season may play a more significant role in controlling summer soil temperature at a depth of 40 cm than the changes in air temperature at Irkutsk, Russia. Summer precipitation is likely to have a cooling effect on soil temperature by increasing surface wetness and soil moisture, thus leads to more energy consumption for evaporation, while rainfall in prewinter may warm soil temperature through the effects of the greater freezing latent heat (Iijima et al., 2010; Park et al., 2013; Westermann et al., 2011; Zhang et al., 2001). In the warmer permafrost region (mean annual ground temperature > −0.5°C at the depth of zero annual amplitude), intensive precipitation in summer results in abrupt rising of soil temperature at shallow depth and an earlier thawing of the active layer, but reduces seasonal variations of soil temperatures and decreases the mean annual soil temperature (Luo et al., 2020). However, in the permafrost regions where the active layer is thin and always at or near saturation, an increase in rainfall during summer may have little impact (Zhang et al., 2001). Nevertheless, rainfall is a key factor controlling active layer thickness (Cao et al., 2017; James et al., 2019; Karjalainen et al., 2019), implying that the active layer may deepen in the future under a warming climate. Consequently, the influences of rainfall on soil temperatures are likely to be strengthened through more significant soil moisture feedback and runoff generation-outflow mechanisms (Eltahir, 1998; Gao et al., 2016; Luo et al., 2003).

Soil moisture has decreased in the seasonal frost region; however, it increased at a large group of sites in the permafrost regions (Figures S3f–S3h). In the frost-related region where soil moisture remains relatively high, it has a greater influence on land-atmosphere heat exchange through freeze-thaw cycles (Cheng & Wu, 2007; Liljedahl et al., 2016; Martin et al., 2019). A study has shown that soil moisture in topsoil layers decreases during summer season (JJA) in the permafrost region (Teufel & Sushama, 2019); thus, an increase in soil moisture at the sites located in the permafrost region can be partially attributable to the increases of rainfall in prewinter season (SON) and active layer thickening (Andresen et al., 2020). Trends in soil moisture significantly and nonlinearly relate to ΔT trends at multiple depths, but thick confidence bands in response curves indicate a large number of uncertainties (Figures 6b–6d). An increase in vegetation leads to a decrease in soil temperature during summer when canopies are present, while the net effect of vegetation on soil temperature remains unclear (Loranty et al., 2018). At decadal scales, it is found that the changes in vegetation have little impact on trends in $\Delta T_{0.2}$ and $\Delta T_{0.8}$, but significantly affect $\Delta T_{1.6}$ trends (Figures 6b–6d). This further implies that greening of vegetation has a cooling effect on the mean annual soil temperature at 1.6 m and mean annual air temperature over the area, which is in line with a recent study in North America (García-García et al., 2019).

5. Conclusions

This study provides the first holistic pictures of long-term trends in soil–atmosphere temperature differences in response to the changing environment at a large spatiotemporal scale. By quantifying trends in ΔT and the role of the environmental alterations from 1981 to 2015 in northern Eurasia, we conclude:

1. The warming rate of soil temperature is generally less than that of air temperature at depths of 0.8 and 1.6 m except for soil temperature at 0.2 m in the seasonal frost region that increases more rapidly than air temperature
2. Inconsistent warming rates of the mean annual air and soil temperatures lead to interannual variations of ΔT, which are spatially heterogeneous across northern Eurasia
3. Changes in snow cover and soil moisture explain a significant portion of the positive trends in ΔT, suggesting that increases in ΔT are mainly associated with alterations in snow cover and soil moisture, especially by snow cover thickness changes. Meanwhile, decreases in ΔT relate to more factors, including the changes in snow cover duration, solar radiation, rainfall, and vegetation

A sparse observation network in such a large area brings uncertainties and may limit implementation of the results. Thus, it is recommended to develop the current database in multilayer soil temperatures, particularly in the continuous permafrost region, and enhance observational networks on the dynamics of soil properties (e.g., soil carbon stock) (which are not visible in our study) to systematically improve our knowledge of mitigated soil-atmosphere temperature difference in a changing world. The findings can improve our understanding of how the changing environment would influence land–climate thermal interactions at decadal scales under future climate change. This is also of relevance and interest in multiple disciplines as temperature regimes at the land-atmosphere interface are fundamental to understanding of subsoil biogeochemical cycles, roots development, and infrastructure stability.

Data Availability Statement

The soil and air temperatures, and snow depth data can be downloaded from the following URL (http://meteo.ru/english/climate/cl_data.php). The gridded data can be downloaded from ERA5-Land product (https://cds.climate.copernicus.eu/cdsapp#!/home).

Acknowledgments
The China Scholarship Council funds to L. Chen. The Academy of Finland funds to J. Aalto and M. Luato (The project numbers: 307761 and 286950).

References

Aalto, J., Scherrer, D., Lenoir, J., Guisan, A., & Luoto, M. (2018). Biogeophysical controls on soil-atmosphere thermal differences: Implications on warming Arctic ecosystems. *Environmental Research Letters*, *13*(7), 074003. https://doi.org/10.1088/1748-9326/aac83e

Andresen, C. G., Lawrence, D. M., Wilson, C. J., McGuire, A. D., Koven, C., Schaefer, K., et al. (2020). Soil moisture and hydrology projections of the permafrost region – A model intercomparison. *The Cryosphere*, *14*(2), 445–459. https://doi.org/10.5194/tc-14-445-2020

Bartlett, M. G., Chapman, D. S., & Harris, R. N. (2004). Snow and the ground temperature record of climate change. *Journal of Geophysical Research*, *109*(F4). https://doi.org/10.1029/2004JF000224

Bartlett, M. G., Chapman, D. S., & Harris, R. N. (2005). Snow effect on North American ground temperatures, 1950–2002. *Journal of Geophysical Research*, *110*(F3). https://doi.org/10.1029/2005JF000293

Bartlett, M. G., Chapman, D. S., & Harris, R. N. (2006). A decade of ground–air temperature tracking at Emigrant Pass Observatory, *Journal of Climate*, *19*(15), 3722–3731. https://doi.org/10.1175/JCLI3808.1

Belsley, D. A., Kuh, E., & Welsch, R. E. (2005). *Regression diagnostics: Identifying influential data and sources of collinearity*. John Wiley & Sons.

Bernal, B., McKinley, D. C., Hungate, B. A., White, P. M., Mozdzer, T. J., & Megonigal, J. P. (2016). Limits to soil carbon stability; Deep, ancient soil carbon decomposition stimulated by new labile organic inputs. *Soil Biology and Biochemistry*, *98*, 85–94. https://doi.org/10.1016/j.soilbio.2016.04.007

Bintanja, R., & Andry, O. (2017). Towards a rain-dominated Arctic. *Nature Climate Change*, *7*(4), 263–267. https://doi.org/10.1038/nclimate3240

Blunden, J., & Arndt, D. S. (2019). State of the climate in 2018. *Bulletin of the American Meteorological Society*, *100*(9), Si–S306. https://doi.org/10.1175/2019BAMSStateoftheClimate.1

Bokhorst, S., Pedersen, S. H., Brucker, L., Anisimov, O., Bjerke, J. W., Brown, R. D., et al. (2016). Changing Arctic snow cover: A review of recent developments and assessment of future needs for observations, modeling, and impacts. *Ambio*, *45*(5), 516–537. https://doi.org/10.1007/s13280-016-0770-0

Breiman, L. (2001). Random Forests. *Machine Learning*, *45*(1), 5–32. https://doi.org/10.1023/A:1010933404324

Brown, J., Sidlauskas, F. J., & Delinski, G. (1997). *Circum-Arctic Map of Permafrost and ground ice conditions [map]. The Survey; for sale by information services*.

Bulygina, O. N., Groisman, P. Y., Razuvaev, V. N., & Korshunova, N. N. (2011). Changes in snow cover characteristics over Northern Eurasia since 1966. *Environmental Research Letters*, *6*(4), 045204. https://doi.org/10.1088/1748-9326/6/4/045204

Bulygina, O. N., & Razuvaev, V. N. (2012). Daily temperature and precipitation data for 518 Russian Meteorological Stations (1881–2010). *Environmental system science data infrastructure for a virtual ecosystem; Carbon Dioxide Information Analysis Center (CDIAC), Oak Ridge National Laboratory (ORNL), Oak Ridge, TN (United States)*. https://doi.org/10.3334/CDIAC/cli.100

Cao, B., Gruber, S., Zhang, T., Li, L., Peng, X., Wang, K., et al. (2017). Spatial variability of active layer thickness detected by ground-penetrating radar in the Qilian Mountains, Western China. *Journal of Geophysical Research: Earth Surface*, *122*(3), 574–591. https://doi.org/10.1002/2016JF004018

Chen, L., Aalto, J., & Luoto, M. (2021). Significant shallow–depth soil warming over Russia during the past 40 years. *Global and Planetary Change*, *197*, 103394. http://doi.org/10.1016/j.gloplacha.2020.103394

Cheng, G., & Wu, T. (2007). Responses of permafrost to climate change and their environmental significance, Qinghai-Tibet Plateau. *Journal of Geophysical Research*, *112*(F2). https://doi.org/10.1029/2006JF000631

Davidson, E. A., & Janssens, I. A. (2006). Temperature sensitivity of soil carbon decomposition and feedbacks to climate change. *Nature*, *440*(7081), 165–173. https://doi.org/10.1038/nature04514

Decharme, B., Brun, E., Boone, A., Delire, C., Le Moigne, P., & Morin, S. (2016). Impacts of snow and organic soils parameterization on northern Eurasian soil temperature profiles simulated by the ISBA land surface model. *The Cryosphere*, *10*(2), 853–877. https://doi.org/10.5194/tc-10-853-2016

Donat, M. G., Lowry, A. L., Alexander, L. V., O'Gorman, P. A., & Maher, N. (2016). More extreme precipitation in the world's dry and wet regions. *Nature Climate Change*, *6*(5), 508–513. https://doi.org/10.1038/nclimate2941

Dormann, C. F., Elith, J., Bacher, S., Buchmann, C., Carl, G., Carré, G., et al. (2013). Collinearity: A review of methods to deal with it and a simulation study evaluating their performance. *Ecography*, *36*(1), 27–46. https://doi.org/10.1111/j.1600-0587.2012.07348.x

Douglass, D. H., Clader, B. D., Christy, J. R., Michaels, P. J., Belsley, D. A. (2003). Test for harmful collinearity among predictor variables used in modeling global temperature. *Climate Research*, *24*, 15–18. http://doi.org/10.3354/cr024015

Eltahir, E. A. B. (1998). A soil moisture–rainfall feedback mechanism: 1. Theory and observations. *Water Resources Research*, *34*(4), 765–776. https://doi.org/10.1029/97WR03499

Fasiolo, M., Nedellec, R., Goude, Y., Capezza, C., & Wood, S. N. (2020). *mgcViz: Visualisations for generalized additive models*. [Computer software]. https://CRAN.R-project.org/package=mgcViz

Frenne, P. D., Zellweger, F., Rodríguez-Sánchez, F., Scheffers, B. R., Hylander, K., Luoto, M., et al. (2019). Global buffering of temperatures under forest canopies. *Nature Ecology & Evolution*, *3*(5), 744. https://doi.org/10.1038/s41559-019-0842-1

Gao, T., Zhang, T., Cao, L., Kang, S., & Sillanpää, M. (2016). Reduced winter runoff in a mountainous permafrost region in the northern Tibetan Plateau. *Cold Regions Science and Technology*, *126*, 36–43. https://doi.org/10.1016/j.coldregions.2016.03.007

García-García, A., Cuesta-Valero, F. J., Beltrami, H., & Smerdon, J. E. (2016). Simulation of air and ground temperatures in PMIP3/CMIP5 last millennium simulations: Implications for climate reconstructions from borehole temperature profiles. *Environmental Research Letters*, *11*(4), 044022. https://doi.org/10.1088/1748-9326/11/4/044022

García-García, A., Cuesta-Valero, F. J., Beltrami, H., & Smerdon, J. E. (2019). Characterization of air and ground temperature relationships within the CMIP5 historical and future climate simulations. *Journal of Geophysical Research: Atmosphere*, *124*(7), 3903–3929. https://doi.org/10.1029/2018JD030117

Gilichinsky, D. A., Barry, R. G., Bykhovets, S. S., Sorokovikov, V. A., Zhang, T., Zudin, S. L., & Fedorov-Davydov, D. G. (1998). A century of temperature observations of soil climate: Methods of analysis and long-term trends. In *Proceedings of 7th International conference on permafrost* (pp. 313–317). Yellowknife. June 23-27, 1998.

González-Rouco, F., Storch, H. v, & Zorita, E. (2003). Deep soil temperature as proxy for surface air-temperature in a coupled model simulation of the last thousand years. *Geophysical Research Letters*, *30*(21). https://doi.org/10.1029/2003GL018264

Groisman, P. Y., Bulygina, O. N., Yin, X., Vose, R. S., Gulev, S. K., Hanssen-Bauer, I., & Førland, E. (2016). Recent changes in the frequency of freezing precipitation in North America and Northern Eurasia. *Environmental Research Letters*, *11*(4), 045007. https://doi.org/10.1088/1748-9326/11/4/045007

Grundstein, A., Todhunter, P., & Mote, T. (2005). Snowpack control over the thermal offset of air and soil temperatures in eastern North Dakota. *Geophysical Research Letters*, *32*(8). https://doi.org/10.1029/2005GL022532

Hair, J. F. J., Black, W. C., Babin, B. J., & Andersen, R. E. (1995). *Multivariate data analysis*. Macmillan.

Hastie, T. J., & Tibshirani, R. J. (1990). *Generalized additive models*. CRC Press.

Hersbach, H., Bell, B., Berrisford, P., Hirahara, S., Horányi, A., Muñoz-Sabater, J., et al. (2020). The ERA5 global reanalysis. *Quarterly Journal of the Royal Meteorological Society*, *146*(730), 1999–2049. https://doi.org/10.1002/qj.3803

Hrbáček, F., Láska, K., & Engel, Z. (2016). Effect of snow cover on the active-layer thermal regime – A case study from James Ross Island, Antarctic Peninsula. *Permafrost and Periglacial Processes*, *27*(3), 307–315. https://doi.org/10.1002/ppp.1871

Iijima, Y., Fedorov, A. N., Park, H., Suzuki, K., Yabuki, H., Maximov, T. C., & Ohata, T. (2010). Abrupt increases in soil temperatures following increased precipitation in a permafrost region, central Lena River basin, Russia. *Permafrost and Periglacial Processes*, *21*(1), 30–41. https://doi.org/10.1002/ppp.662

Isaksen, K., Ødegård, R. S., Etzelmüller, B., Hilbich, C., Hauck, C., Farbrot, H., et al. (2011). Degrading mountain permafrost in southern Norway: Spatial and temporal variability of mean ground temperatures, 1999–2009. *Permafrost and Periglacial Processes*, *22*(4), 361–377. https://doi.org/10.1002/ppp.728

James, S. R., Knox, H. A., Abbott, R. E., Panning, M. P., & Screaton, E. J. (2019). Insights into permafrost and seasonal active-layer dynamics from ambient seismic noise monitoring. *Journal of Geophysical Research: Earth Surface*, *124*(7), 1798–1816. https://doi.org/10.1029/2019JF005051

Jobbágy, E. G., & Jackson, R. B. (2000). The vertical distribution of soil organic carbon and its relation to climate and vegetation. *Ecological Applications*, *10*(2), 423–436. https://doi.org/10.1890/1051-0761(2000)010[0423:TVDOSO]2.0.CO;2

Jungqvist, G., Oni, S. K., Teutschbein, C., & Futter, M. N. (2014). Effect of climate change on soil temperature in Swedish boreal forests. *PloS One*, *9*(4). e93957. https://doi.org/10.1371/journal.pone.0093957

Karjalainen, O., Luoto, M., Aalto, J., & Hjort, J. (2019). New insights into the environmental factors controlling the ground thermal regime across the Northern Hemisphere: A comparison between permafrost and non-permafrost areas. *The Cryosphere*, *13*(2), 693–707. https://doi.org/10.5194/tc-13-693-2019

Kassambara, A. (2020). *Ggpubr: "ggplot2" based publication ready plots*. [Computer software]. https://CRAN.R-project.org/package=ggpubr

Knapp, A. K., Beier, C., Briske, D. D., Classen, A. T., Luo, Y., Reichstein, M., et al. (2008). Consequences of more extreme precipitation regimes for terrestrial ecosystems. *BioScience*, *58*(9), 811–821. https://doi.org/10.1641/B580908

Knight, J. H., Minasny, B., McBratney, A. B., Koen, T. B., & Murphy, B. W. (2018). Soil temperature increase in eastern Australia for the past 50years. *Geoderma*, *313*, 241–249. https://doi.org/10.1016/j.geoderma.2017.11.015

Koven, C. D., Lawrence, D. M., & Riley, W. J. (2015). Permafrost carbon–climate feedback is sensitive to deep soil carbon decomposability but not deep soil nitrogen dynamics. *Proceedings of the National Academy of Sciences*, *112*(12), 3752–3757. https://doi.org/10.1073/pnas.1415123112

Lenoir, J., Hattab, T., & Pierre, G. (2017). Climatic microrefugia under anthropogenic climate change: Implications for species redistribution. *Ecography*, *40*(2), 253–266. https://doi.org/10.1111/ecog.02788

Liljedahl, A. K., Boike, J., Daanen, R. P., Fedorov, A. N., Frost, G. V., Grosse, G., et al. (2016). Pan-Arctic ice-wedge degradation in warming permafrost and its influence on tundra hydrology. *Nature Geoscience*, *9*(4), 312–318. https://doi.org/10.1038/ngeo2674

Loranty, M. M., Abbott, B. W., Blok, D., Douglas, T. A., Epstein, H. E., Forbes, B. C., et al. (2018). Reviews and syntheses: Changing ecosystem influences on soil thermal regimes in northern high-latitude permafrost regions. *Biogeosciences*, *15*(17), 5287–5313. https://doi.org/10.5194/bg-15-5287-2018

Luo, D., Jin, H., Bense, V. F., Jin, X., & Li, X. (2020). Hydrothermal processes of near-surface warm permafrost in response to strong precipitation events in the Headwater Area of the Yellow River, Tibetan Plateau. *Geoderma*, *376*, 114531. https://doi.org/10.1016/j.geoderma.2020.114531

Luo, D., Jin, H., Marchenko, S. S., & Romanovsky, V. E. (2018). Difference between near-surface air, land surface and ground surface temperatures and their influences on the frozen ground on the Qinghai-Tibet Plateau. *Geoderma*, *312*, 74–85. https://doi.org/10.1016/j.geoderma.2017.09.037

Luo, L., Robock, A., Vinnikov, K. Y., Schlosser, C. A., Slater, A. G., Boone, A., et al. (2003). Effects of frozen soil on soil temperature, spring infiltration, and runoff: Results from the PILPS 2(d) experiment at Valdai, Russia. *Journal of Hydrometeorology*, *4*(2), 334–351. https://doi.org/10.1175/1525-7541(2003)4<334:EOFSOS>2.0.CO;2

Martin, L. C. P., Nitzbon, J., Aas, K. S., Etzelmüller, B., Kristiansen, H., & Westermann, S. (2019). Stability conditions of peat plateaus and palsas in northern Norway. *Journal of Geophysical Research: Earth Surface*, *124*(3), 705–719. https://doi.org/10.1029/2018JF004945

Papalexiou, S. M., & Montanari, A. (2019). Global and regional increase of precipitation extremes under global warming. *Water Resources Research*, *55*(6), 4901–4914. https://doi.org/10.1029/2018WR024067

Park, H., Walsh, J., Fedorov, A. N., Sherstiukov, A. B., Iijima, Y., & Ohata, T. (2013). The influence of climate and hydrological variables on opposite anomaly in active-layer thickness between Eurasian and North American watersheds. *The Cryosphere*, *7*(2), 631–645. https://doi.org/10.5194/tc-7-631-2013

Patterson, H. D., & Thompson, R. (1971). Recovery of inter-block information when block sizes are unequal. *Biometrika*, *58*(3), 545–554. JSTOR. https://doi.org/10.2307/2334389

Peng, S., Ciais, P., Krinner, G., Wang, T., Gouttevin, I., McGuire, A. D., et al. (2016). Simulated high-latitude soil thermal dynamics during the past 4 decades. *The Cryosphere*, *10*(1), 179–192. https://doi.org/10.5194/tc-10-179-2016

Putnam, S. N., & Chapman, D. S. (1996). A geothermal climate change observatory: First year results from Emigrant Pass in northwest UT *Journal of Geophysical Research*, *101*(B10), 21877–21890. https://doi.org/10.1029/96JB01903

R core team (2017). *R: A language and environment for statistical computing*. Vienna: R Foundation for Statistical Computing. https://www.r-project.org/

Romanovsky, V. E., Sazonova, T. S., Balobaev, V. T., Shender, N. I., & Sergueev, D. O. (2007). Past and recent changes in air and permafrost temperatures in eastern Siberia. *Global and Planetary Change*, *56*(3), 399–413. https//doi.org/10.1016/j.gloplacha.2006.07.022

Sherstiukov, A. (2012). *Статистический контроль массива суточных данных температуры почвогрунтов (Statistical quality control of soil temperature dataset) (No. 176)* (pp. 224–232). http://meteo.ru/index.php?option=com_docman&task=doc_download&gid=107

Teufel, B., & Sushama, L. (2019). Abrupt changes across the Arctic permafrost region endanger northern development. *Nature Climate Change*, *9*(11), 858–862. https://doi.org/10.1038/s41558-019-0614-6

Thuiller, W., Georges, D., Engler, R., & Breiner, F. (2020). *biomod2: Ensemble platform for species distribution modeling (3.4.6)*. Computer software. https://CRAN.R-project.org/package=biomod2

Thuiller, W., Lafourcade, B., Engler, R., & Araújo, M. B. (2009). BIOMOD – A platform for ensemble forecasting of species distributions. *Ecography*, *32*(3), 369–373. https://doi.org/10.1111/j.1600-0587.2008.05742.x

Walther, G.-R., Post, E., Convey, P., Menzel, A., Parmesan, C., Beebee, T. J. C., et al. (2002). Ecological responses to recent climate change. *Nature*, *416*(6879), 389–395. https://doi.org/10.1038/416389a

Wang, Y., Hu, Z.-Z., & Yan, F. (2017). Spatiotemporal variations of differences between surface air and ground temperatures in China. *Journal of Geophysical Research: Atmosphere*, *122*(15), 7990–7999. https://doi.org/10.1002/2016JD026110

Wang, X., Piao, S., Ciais, P., Li, J., Friedlingstein, P., Koven, C., & Chen, A. (2011). Spring temperature change and its implication in the change of vegetation growth in North America from 1982 to 2006. *Proceedings of the National Academy of Sciences*, *108*(4), 1240–1245. https://doi.org/10.1073/pnas.1014425108

Westermann, S., Boike, J., Langer, M., Schuler, T. V., & Etzelmüller, B. (2011). Modeling the impact of wintertime rain events on the thermal regime of permafrost. *The Cryosphere*, *5*(4), 945–959. https://doi.org/10.5194/tc-5-945-2011

Wickham, H., Chang, W., Henry, L., Pedersen, T. L., Takahashi, K., Wilke, C., et al. (2020). *ggplot2: Create elegant data visualisations Using the Grammar of graphics* (3.3.0). [Computer software]. https://CRAN.R-project.org/package=ggplot2

Wickham, H., François, R., Henry, L., Müller, K., & RStudio (2020). *Dplyr: A grammar of data manipulation (0.8.5)*. [Computer software]. https://CRAN.R-project.org/package=dplyr

Wilke, C. O. (2019). *cowplot: Streamlined plot Theme and plot Annotations for "ggplot2" (1.0.0)*. [Computer software]. https://CRAN.R-project.org/package=cowplot

Wood, S. (2019). *mgcv: Mixed GAM computation vehicle with automatic smoothness estimation (1.8-31)*. [Computer software]. https://CRAN.R-project.org/package=mgcv

Wood, S. N. (2017). *Generalized additive models: An introduction with R* (2nd ed.). CRC Press.

Yazaki, T., Iwata, Y., Hirota, T., Kominami, Y., Kawakata, T., Yoshida, T., et al. (2013). Influences of winter climatic conditions on the relation between annual mean soil and air temperatures from central to northern Japan. *Cold Regions Science and Technology*, *85*, 217–224. https://doi.org/10.1016/j.coldregions.2012.09.009

Zhang, T. (2005). Influence of the seasonal snow cover on the ground thermal regime: An overview. *Reviews of Geophysics*, *43*(4). https://doi.org/10.1029/2004RG000157

Zhang, T., Barry, R. G., Gilichinsky, D., Bykhovets, S. S., Sorokovikov, V. A., & Ye, J. (2001). An amplified signal of climatic change in soil temperatures during the last century at Irkutsk, Russia. *Climatic Change*, *49*(1), 41–76. https://doi.org/10.1023/A:1010790203146

Zhang, Y., Sherstiukov, A. B., Qian, B., Kokelj, S. V., & Lantz, T. C. (2018). Impacts of snow on soil temperature observed across the circumpolar north. *Environmental Research Letters*, *13*(4), 044012. https://doi.org/10.1088/1748-9326/aab1e7